

## 1 Introduction

### Complex Langevin (CL) equation:

$$\text{Re}\dot{z}(\theta) = \text{Re}K(z(\theta)) + \eta(\theta), \quad \text{Drift term: } K(z) = i\frac{dS}{dz}, \quad z \in \mathcal{M}_C = \mathbb{C}^N,$$

$$\text{Im}\dot{z}(\theta) = \text{Im}K(z(\theta)), \quad \text{Noise term: } \langle \eta(\theta) \rangle = 0, \quad \langle \eta(\theta)\eta(\theta') \rangle = 2\delta(\theta - \theta')$$

- Complex Fokker-Planck equation, complexification of degrees of freedom
- This allows us to compute oscillatory integrals:

$$\langle \mathcal{O} \rangle = \frac{1}{Z} \int dx \mathcal{O}(x) \exp[iS(x)] \approx \lim_{\theta_0 \rightarrow \infty} \frac{1}{T} \int_{\theta_0}^{\theta_0+T} d\theta \mathcal{O}[z(\theta)]$$

- CL suffers from instabilities:
  - Runaway instabilities → avoided by an adaptive stepsize
  - Wrong convergence → mitigated by stabilization techniques → improvements investigated here
- We introduce a CL step for anisotropic lattices

## 2 Complex Langevin for real-time Yang-Mills simulations

- Complexification of the Lie algebra of the gauge group:  $SU(N) \rightarrow SL(N, \mathbb{C})$
- Complex Langevin equation for Yang-Mills theories (continuum  $S_{\text{YM}}$ ):

$$\frac{\partial A_\mu^a(\theta, x)}{\partial \theta} = i \frac{\delta S_{\text{YM}}}{\delta A_\mu^a(\theta, x)} + \eta_\mu^a(\theta, x), \quad S_{\text{YM}} = -\frac{1}{4} \int_{\mathcal{E}} d^4x F_a^{\mu\nu} F_{\mu\nu}^a$$

$$\langle \eta_\mu^a(\theta, x) \rangle = 0, \quad \langle \eta_\mu^a(\theta, x) \eta_\nu^b(\theta', y) \rangle = 2\delta(\theta - \theta') \delta^{(d)}(x - y) \delta^{ab} \delta_{\mu\nu}.$$

- CL step using anisotropic  $a_\mu$  (discrete  $S_W$  on  $N_t \times N_s^3$  lattice):

$$U'_{x\mu} = \exp[-i\lambda_a(\epsilon_\mu D_{x,\mu}^a S_W[U] - \sqrt{\epsilon_\mu} \eta_{x,\mu}^a)] U_{x\mu}, \quad \epsilon_0 = \epsilon \frac{|a_t|^2}{a_s^2}, \quad \epsilon_i = \epsilon$$

- Our observation:** Partial continuum limit with  $|a_t| \ll a_s$  and  $N_t|a_t| = \text{const.}$  improves convergence for real-time CL-simulations

## 4 Progress on the stabilization of real-time YM simulations

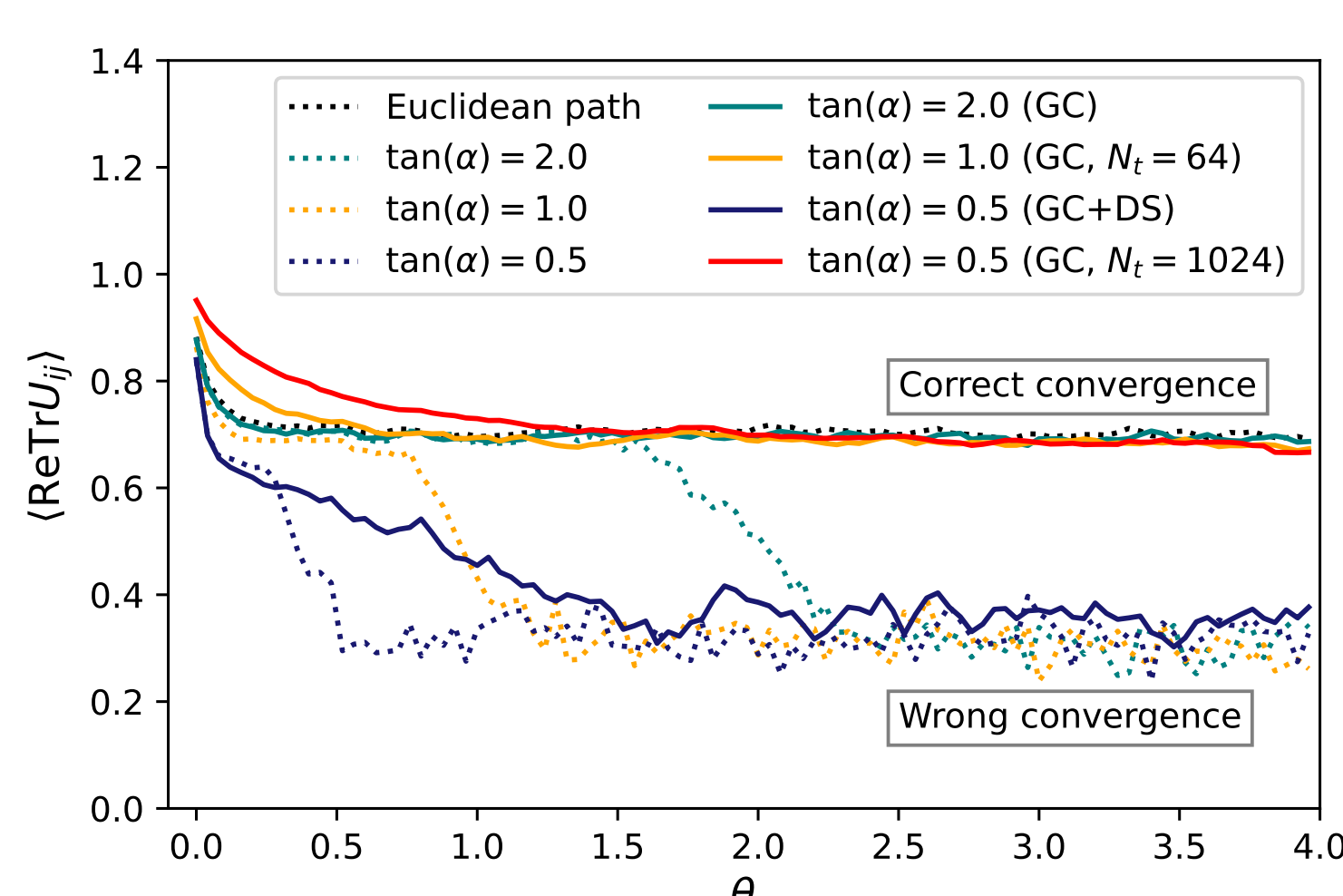


Figure 2:  $\langle \mathcal{O} \rangle$  for different contour tilt angles of  $\mathcal{C}_0$  and stabilization techniques. If not mentioned otherwise  $N_t = 16$ .

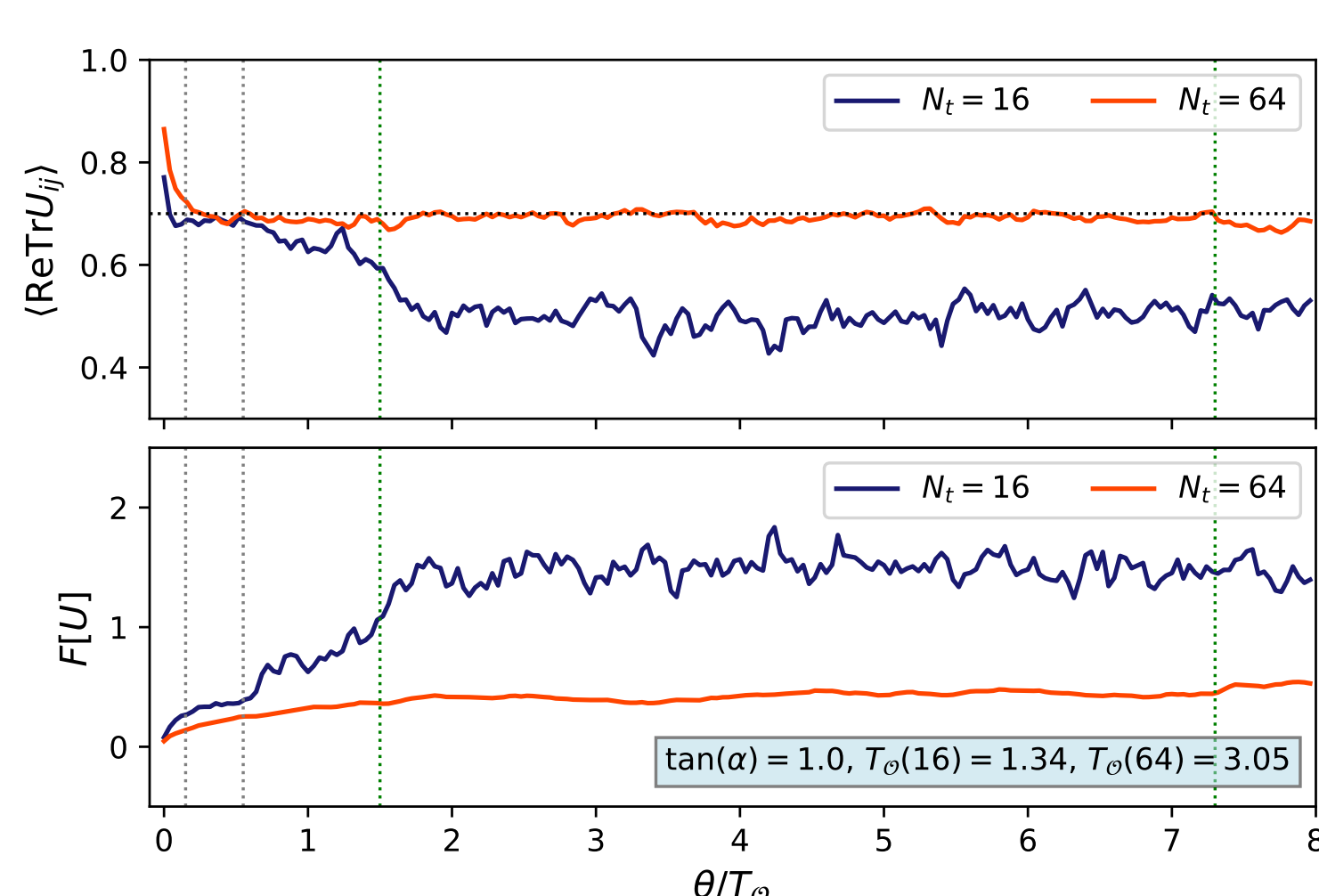


Figure 3: Observable (top) and unitarity norm (bottom) as functions of rescaled Langevin time (AS + GC, no DS).

Fig. 2 reproduces results of [1] for the average spatial plaquette ( $\mathcal{O} = \text{ReTr}U_{ij}$ ). We use AS (always), GC and DS to overcome runaways and wrong convergence.

- $\mathcal{O}$  without stabilization: short stability region or wrong convergence
- $\langle \mathcal{O} \rangle$  should be ind. of contour (time transl. inv.)
- Stabilization techniques and partial continuum limit improve convergence
- DS can improve stability but introduces bias
- Autocorrelation time grows with increasing  $N_t$

Fig. 3 shows CL evolution scaled by the autocorr. time.

- Stable  $\theta$ -region grows faster with  $N_t$  than  $T_{\mathcal{O}}$
- No dynamical stabilization is needed ⇒ biased results are avoided
- Novel  $\epsilon_\mu$  prescription in CL step effectively enlarges stable  $\theta$ -region

## 5 Conclusion

- Stabilization techniques extend the applicability of CL by mitigating known instabilities
- Anisotropic lattice discretization can enlarge the stable  $\theta$ -regions
- Stability region increases faster with respect to  $N_t$  than the autocorrelation time  $T_{\mathcal{O}}$
- ⇒ Extrapolation to Schwinger-Keldysh contour might be possible
- ⇒ Application to real-time observables

### References:

- [1] Berges, J. et al. (2007). PRD, 75, 045007. [arXiv:0609058]
- [2] Aarts, G. et al. (2010). PLB, 687(2–3), 154–159. [arXiv:0912.3360]
- [3] Seiler, E., Sexty, D., Stamatescu, I.-O. (2013). PLB, 723(1–3), 213–216. [arXiv:1211.3709]
- [4] Attanasio, F., Jäger, B. (2019). EPJC, 79(1), 16. [arXiv:1808.04400]

## 3 Methods

- Path integral is regularized by tilting the time contour
- Our focus:** Stabilizing the tilted part of the contour

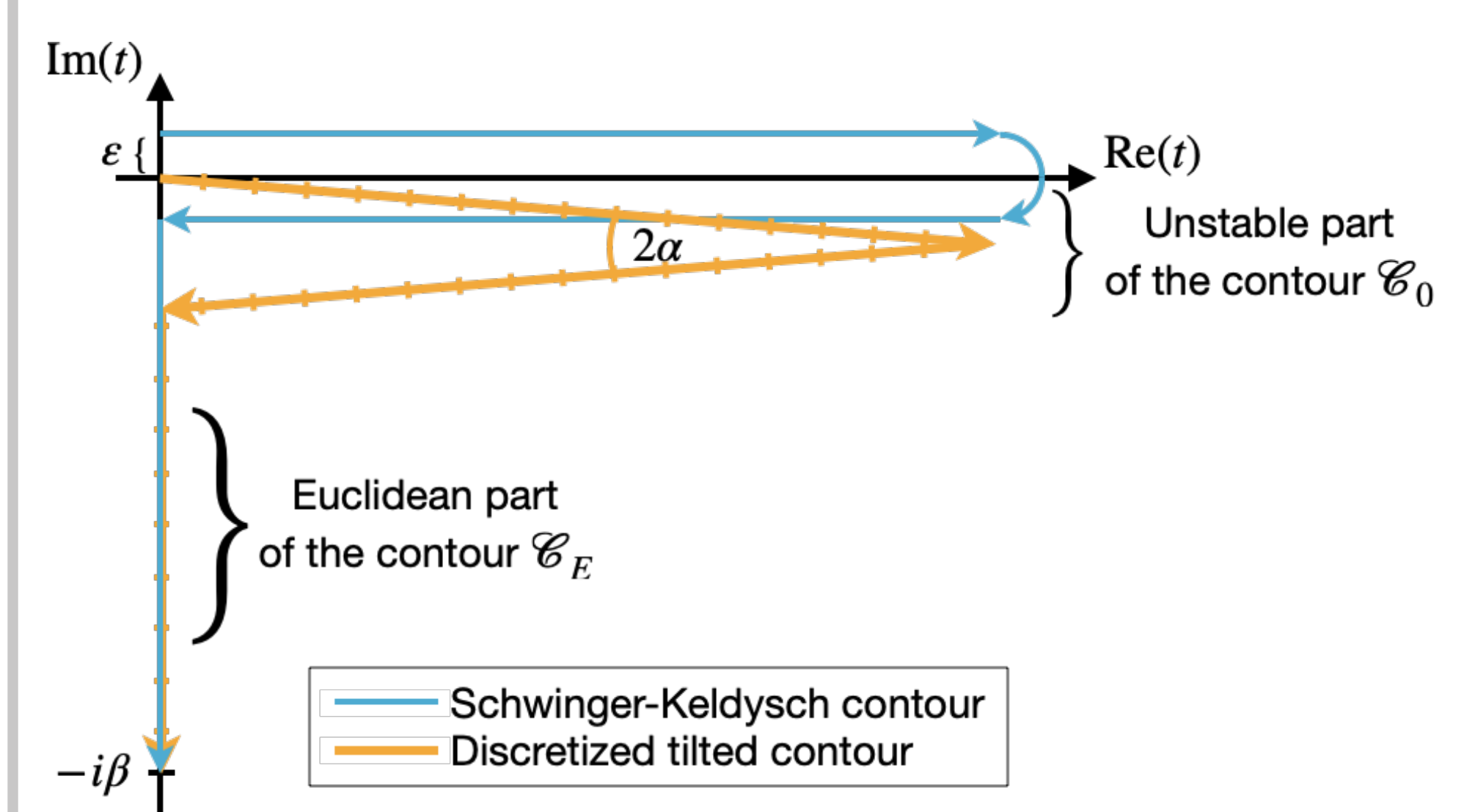


Figure 1: Cont. and discr. Schwinger-Keldysh contour.

### Modern stabilization techniques:

- Adaptive stepsize (AS) [2]** counteracts runaways:

$$\epsilon \mapsto \tilde{\epsilon} = \epsilon \frac{B}{\max_{x,\mu,a} |K_{x,\mu}^a|}$$

- Gauge cooling (GC) [3]** reduces “distance”  $F[U]$  to the  $SU(N)$  group:

$$U_{x,\mu} \mapsto U_{x,\mu}^V = V_{x,\mu} U_{x,\mu} V_{x+\mu,\mu}^{-1},$$

$$F[U] = \sum_{x,\mu} \text{Tr} [(U_{x,\mu} U_{x,\mu}^\dagger - 1)^2] \rightarrow \min$$

- Dynamical stabilization (DS) [4]** reduces excursions to  $SL(N)$ :

$$K_{x,\mu}^a \mapsto \tilde{K}_{x,\mu}^a = K_{x,\mu}^a + i\alpha M_x^a,$$

$$M_x^a \propto F[U], \quad \frac{d\mathcal{O}}{d\alpha} \approx 0$$

### Sampling uncorrelated measurements: autocorrelation time

- Autocorrelation function:**

$$R_{\mathcal{O}}(\tau) = \frac{\langle (\mathcal{O}_\theta - \langle \mathcal{O}_\theta \rangle) (\mathcal{O}_{\theta+\tau} - \langle \mathcal{O}_{\theta+\tau} \rangle) \rangle}{\sigma_{\mathcal{O}} \sigma_{\theta+\tau}}$$

- Autocorrelation time  $T_{\mathcal{O}}$ :**

$$R_{\mathcal{O}}(\tau) \approx \exp(-\tau/T_{\mathcal{O}})$$